Annals of Botany **101**: 983–995, 2008
doi:10.1093/aob/mcn022, available online at www.aob.oxfordjournals.org

OXFORD JOURNALS
OXFORD UNIVERSITY PRESS

Cellular Ultrastructure and Crystal Development in *Amorphophallus* (Araceae)

CHRISTINA J. PRYCHID[1,*], RACHEL SCHMIDT JABAILY[2] and PAULA J. RUDALL[1]

[1]*Jodrell Laboratory, Royal Botanic Gardens, Kew, Richmond, Surrey, TW9 3DS, UK and* [2]*College of Letters and Science, Botany Unit, 256 Birge Hall, 430 Lincoln Drive, University of Wisconsin, Madison, WI 53706, USA*

Received: 20 November 2007 Returned for revision: 3 January 2008 Accepted: 22 January 2008 Published electronically: 19 February 2008

• *Background and Aims* Species of Araceae accumulate calcium oxalate in the form of characteristically grooved needle-shaped raphide crystals and multi-crystal druses. This study focuses on the distribution and development of raphides and druses during leaf growth in ten species of *Amorphophallus* (Araceae) in order to determine the crystal macropatterns and the underlying ultrastructural features associated with formation of the unusual raphide groove.
• *Methods* Transmission electron microscopy (TEM), scanning electron microscopy (SEM) and both bright-field and polarized-light microscopy were used to study a range of developmental stages.
• *Key Results* Raphide crystals are initiated very early in plant development. They are consistently present in most species and have a fairly uniform distribution within mature tissues. Individual raphides may be formed by calcium oxalate deposition within individual crystal chambers in the vacuole of an idioblast. Druse crystals form later in the true leaves, and are absent from some species. Distribution of druses within leaves is more variable. Druses initially develop at leaf tips and then increase basipetally as the leaf ages. Druse development may also be initiated in crystal chambers.
• *Conclusions* The unusual grooved raphides in *Amorphophallus* species probably result from an unusual crystal chamber morphology. There are multiple systems of transport and biomineralization of calcium into the vacuole of the idioblast. Differences between raphide and druse idioblasts indicate different levels of cellular regulation. The relatively early development of raphides provides a defensive function in soft, growing tissues, and restricts build-up of dangerously high levels of calcium in tissues that lack the ability to adequately regulate calcium. The later development of druses could be primarily for calcium sequestration.

Key words: *Amorphophallus*, Araceae, calcium oxalate, crystals, development, druses, raphides, ultrastructure.

INTRODUCTION

Calcium oxalate crystals occur in different forms throughout the Plant Kingdom. They perform various functions, including herbivory deterrence (Sakai *et al.*, 1984; Hudgins *et al.*, 2003), calcium regulation (Franceschi, 1989; Kostman and Franceschi, 2000; Pennisi and McConnell, 2001; Volk *et al.*, 2002) and are associated with heavy metal tolerance (Franceschi and Nakata, 2005). They are categorized into several morphological types: raphides, druses, styloids, prisms and crystal sand (reviewed by Franceschi and Horner, 1980; Horner and Wagner, 1995; Prychid and Rudall, 1999; Franceschi and Nakata, 2005). Raphides are bundles of needle-like crystals that represent the most common crystal type in monocots. By contrast, druses (cluster crystals) are roughly spherical aggregates of crystals that occur in only a few early-divergent monocot families, but are common in eudicots and early-divergent angiosperms.

Crystal characters can represent useful synapomorphies for particular plant groups. One striking example is the species-rich and predominantly tropical monocot family Araceae, which belongs to the early-divergent monocot order Alismatales. Both raphides and druses are often concentrated in the mesophyll tissues of Araceae, although other crystal types can also occur (Genua and Hillson, 1985; Mayo *et al.*, 1997; Keating, 2003, 2004). Members of this family possess highly unusual grooved raphide crystals that appear as a 'H' or dumb-bell in cross section (Arnott and Pautard, 1970; Prychid and Rudall, 1999; Kostman and Franceschi, 2000). The only other known occurrence of a grooved crystal is in *Tragia* (Euphorbiaceae); crystals present in the stinging hairs possess a single groove that has been suggested to transport a toxic protein into the wound created by the crystal (Thurston, 1976). Here, we investigate the ontogeny of both raphide and druse crystals in leaves of ten species of *Amorphophallus* (Araceae). Our primary goal is to trace raphide development from a pre-idioblast to a mature crystal in order to visualize the membrane system associated with crystal formation; this will help us to evaluate the formation of the unusual raphide grooves. A secondary goal is to determine whether there is any correlation between the age of the plant tissue and the type and distribution of crystals, as suggested by Volk *et al.* (2002).

There have been relatively few developmental studies carried out on plant crystals, apart from investigations on raphide idioblasts in *Typha angustifolia* (Typhaceae; Horner *et al.*, 1981; Kausch and Horner, 1983), *Lemna minor* (Araceae; Mazen *et al.*, 2003) and *Vitis* (Vitaceae; Webb *et al.*, 1995). Our developmental observations allow us to speculate on the possible structures controlling the formation of the characteristic crystal morphologies.

* For correspondence. E-mail c.prychid@kew.org

TABLE 1. *Material examined. HK indicates material grown at Kew, followed by accession number*

Specimen	Tissue
Amorphophallus bulbifer Blume, HK 1990−994	Embryonic tissue from ungerminated seed
	Young shoots from germinated seed
A. dunnii Tutcher, HK 1978−2290	Mature leaves
A. gallaensis N.E.Br., HK 1956−32601	Mature leaves
A. konjac K.Koch, HK 1998−3419, HK 1997−111, HK 1997−112	Young shoots from tuber
	Young leaves
	Mature leaves
A. krausei Engl., HK 1997−3547	Young shoots from tuber
	Young leaves
	Mature leaves
A. paeoniifolius (Dennst.) Nicolson, HK 1994−3577	Mature leaves
A. salmoneus W.L.A. Hetterscheid, HK 1997−115	Young leaves
	Mature leaves
A. sutepensis Gagnep., HK 1997−109	Mature leaves
A. taurostigma Ittenb., Hett. & Bogner, HK 1994–3548	Mature leaves
A. titanum Becc., HK 1995−3721	Mature leaves
A. variabilis Blume, HK 1997−110	Young shoots from tuber
	Young leaves
	Mature leaves

MATERIALS AND METHODS

Plant material

Material examined was obtained from the living collections at the Royal Botanic Gardens, Kew (Table 1). Leaf material was collected at various ages, from embryonic tissue and germinated seeds to fully mature leaves. Mature *Amorphophallus* usually possess a solitary leaf with a blade that is trisect, with primary divisions that are pinnatisect, bipinnatisect or dichotomously further divided. For this study, mature leaf tips are the tips of the divisional lobes and leaf bases correspond to lobe bases. A young leaf is defined as an unfurled trisect leaf, prior to primary division, with the leaf tip and base being the tip and base of each trisect. This also applies to furled seedling leaves. Embryonic tissue was taken from berries harvested from mature infructescences.

Light microscopy

Material was fixed in formalin–acetic-alcohol (FAA) and stored in 70 % ethanol. After washing in distilled water, leaves were immersed in 0·5 % NaOH and placed in a warm (approx. 50 °C) oven until the tissues were transparent. The leaves were then taken through a graded ethanol series, into Histoclear, and then mounted onto microscope slides in Distrene-dibutyl phthalate-xylene (DPX). Slides were examined using a Leica DMLB photomicroscope fitted with crossed polarizers and a Zeiss Axiocam digital camera.

Transmission electron microscopy

Material was dissected into approx. 2-mm^3 pieces under Karnovsky's fixative and left in fixative overnight at 4 °C. Samples were washed in 0·05 M phosphate buffer before being post-fixed in 1 % osmium tetroxide for two hours at room temperature, washed again in buffer, and dehydrated through a graded ethanol series. Samples were embedded in medium-grade LR White Resin in gelatine capsules. Sectioning was carried out using a Reichert Ultracut microtome. Ultra-thin (silver–gold) sections were cut using a diamond knife, mounted onto formvar-coated slot grids, stained with uranyl acetate and lead citrate in an LKB Ultrostainer, and examined using a JEOL JEM-1210 transmission electron microscope (TEM) at 80 kV.

Scanning electron microscopy

Material was fixed in an identical manner to that for transmission electron microscopy, dehydrated in a graded ethanol series to 100 % ethanol and then critical-point dried using a Tousimis critical-point dryer. Crystals were also isolated from fresh leaves by macerating the tissues in 100 % ethanol, filtering through muslin and air-drying. Samples were mounted onto pin stubs, coated with platinum using an Emitech K550 sputter coater, and examined using a Hitachi cold-field emission scanning electron microscope (SEM) S-4700 at 2 kV.

RESULTS

Distribution and developmental timing of crystal types is variable

Two distinct types of crystal idioblasts occur in the *Amorphophallus* species observed: (1) cells containing grooved raphide crystals (Fig. 1A–G), and (2) cells that contain a single large or several smaller multi-faceted druses (Fig. 1I, J). Each of these two specialized cells produces only one crystal type.

(1) *Raphide idioblasts*. Raphide idioblasts vary in size but at maturity are generally large (up to 200 μm long by 50 μm wide), thin-walled, axially elongated and roughly cylindrical cells, each containing a sack of numerous needle-like crystals that are similarly orientated along the long axis of the cell (Fig. 1A–C). In some cases the ends of the idioblasts are pointed or blunt and project into intercellular spaces, the remainder of the cell being held loosely by mesophyll cells (Fig. 1A). In other cases, the raphide idioblasts are firmly embedded in the surrounding tissue. The crystal bundle can extend almost the full length of the idioblast or can be significantly shorter and embedded in mucilage (Fig. 1C). Raphide crystals vary in size and number per bundle from approx. 100 to 800+ (Fig. 2E). Individual raphides have a fairly constant thickness along their length and taper sharply to points at their tips (Fig. 1D–F). Each crystal has two opposing grooves, which run almost the entire length of the crystal apart from at the midpoint, occasionally at other points along the faces and at the tips (Fig. 1E–G). Barbs or hooks have been seen on

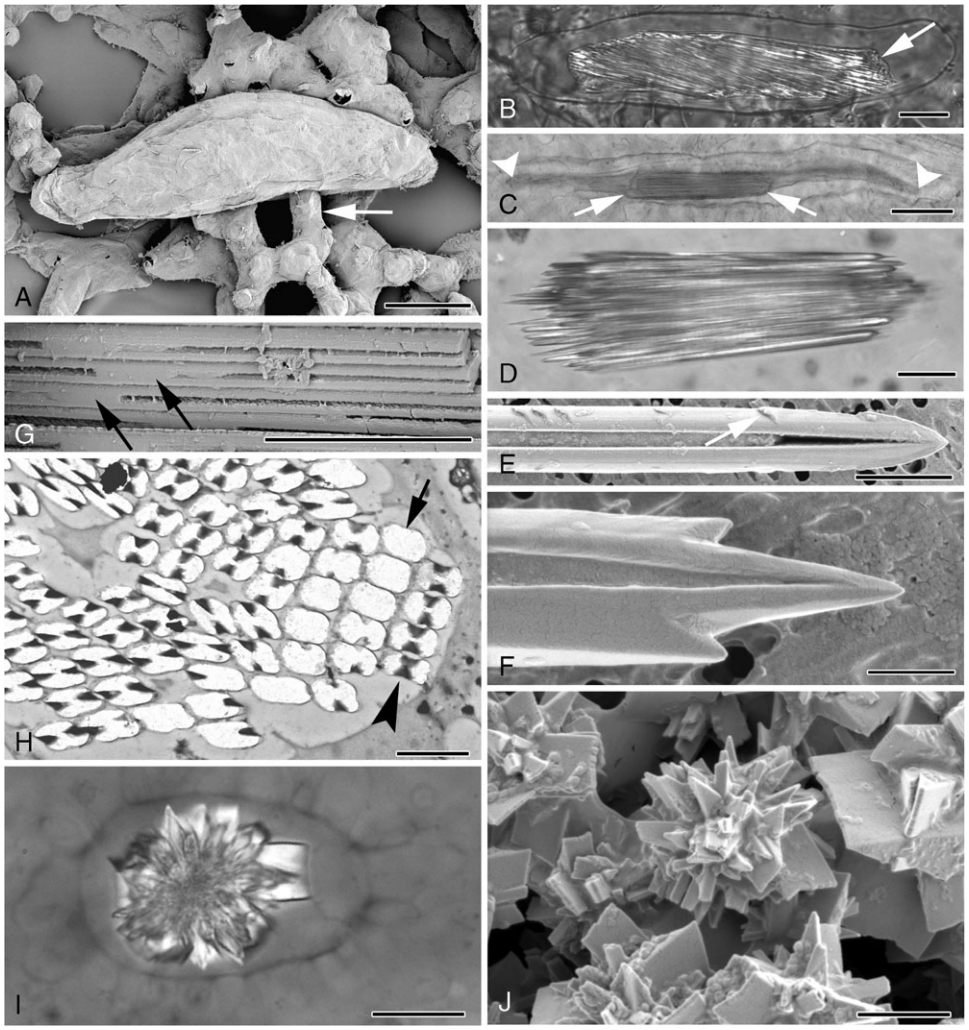

FIG. 1. (A–J) Light and electron micrographs of cell inclusions in *Amorphophallus*. (A) Elongated raphide idioblast in leaf tissue of *A. titanum*. Arrow points to adjacent mesophyll cell. (B) Polarized-light image of a raphide idioblast of *A. variabilis*. Crystals are contained within the cell vacuole (arrowed). (C) Raphide bundle (arrowed) in *A. konjac*, significantly shorter than the length of the cell vacuole, marked by arrowheads. (D) Individual raphide crystals in *A. konjac* taper to pointed tips. (E) Barbs (arrowed) can be seen along the length of a raphide of *A. salmoneus*. One of the two characteristic grooves running the length of the crystal can be seen. (F) Additional points are present on either side of the pointed end of a raphide of *A. salmoneus*. (G) The crystal grooves disappear around the mid-point of each needle, as here in *A. konjac*. (H) Transverse section through a raphide bundle of *A. bulbifer*. At mid-point of crystals absence of groove results in rectangular crystal outlines (arrow), whereas at other points along the crystals the outlines are characteristically H-shaped (arrowhead). (I) Polarized-light image of a druse of *A. salmoneus*. (J) Druse in *A. salmoneus*, numerous crystal faces amalgamated together around a central region. Scale bars: (A, C) = 50 μm; (B, D, I) = 20 μm; (E, H) = 2 μm; (F, J) = 1 μm; (G) = 5 μm.

raphides of *A. salmoneus* and *A. taurostigma* (Fig. 1E, F) but this character is variable, appearing on raphides in some bundles but not in others of the same sample. In crystals that lack grooves, the outline is roughly rectangular with rounded corners, but in grooved crystals the outline is rounded H-shaped or dumb-bell shaped (Fig. 1H).

The distribution of both raphide and druse idioblasts varies even within a species but some general patterns occur. Raphides are present at all stages of leaf development from embryonic tissues to fully mature leaves (except in *A. sutepensis*, which lacks both raphides and druses). Generally, at leaf maturity raphides can be found throughout the leaf, fairly regularly spaced apart within the reticulate venation (Fig. 2A, D). However, in *A. salmoneus* raphides were absent from the mature leaf tips; they initially developed in leaf-base tissues of young leaves and later formed in the mid sections of the leaves (Fig. 2A, B). By contrast, in *A. konjac* and *A. krausei* numerous raphide idioblasts were present throughout the tissues of both young and old leaves, including the leaf tips (Fig. 2C–E).

Idioblasts were generally orientated in the same direction as the closest veins, towards the leaf margin (Fig. 2D, I). *Amorphophallus konjac*, *A. krausei* and *A. variabilis* also possessed a row of raphides between the looped marginal vein and the margin (Fig. 2H).

(2) *Druse idioblasts*. Druse idioblasts generally resemble adjacent cells in size (up to 60 μm in diameter) and shape (Fig. 1I). The druses within them vary in number

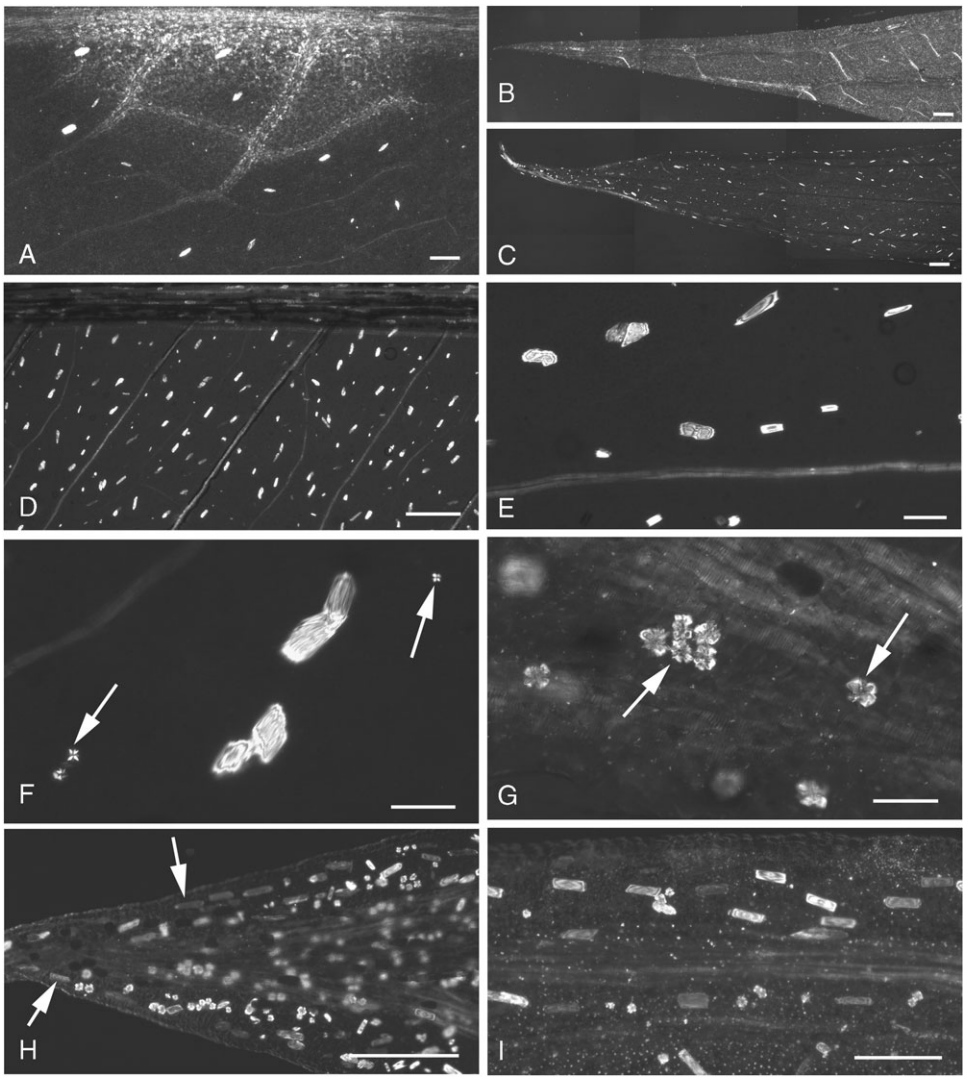

FIG. 2. (A–I) Polarized-light micrographs of cleared mature leaf tissue in *Amorphophallus*. (A) *A. salmoneus*, raphide bundles occur fairly uniformly throughout leaf base. (B) *A. salmoneus*, no raphide idioblasts observed at leaf tip. (C) *A. konjac*, raphides clearly present at leaf tip. (D) *A. konjac*, regularly spaced raphide idioblasts in leaf base. (E) *A. konjac*, leaf base, raphide bundles varying in size. (F) *A. konjac*, druses (arrowed) in leaf base, much smaller than those in leaf tip. (G) *A. konjac*, leaf tip contains large druses (arrowed). (H) *A. variabilis*, leaf tip, raphide bundles (arrowed) can faintly be seen running parallel to the leaf lamina. (I) *A. variabilis*, raphides orientated with their long axes parallel with the adjacent vein. Scale bars: (A, I) = 200 μm; (B–D, H) = 400 μm; (E–G) = 50 μm.

and size, from one or several small crystals, a couple of micrometers in diameter, through to single large crystals, up to 50 μm in width. Each druse is an aggregate of many interlocking crystals of variable morphologies (Fig. 1J).

Druses were not seen in embryonic tissue but were first observed at seedling leaf development of *A. krausei*. At maturity most leaves possess druses, somewhere in their tissues. Druses may be so abundant that almost every cell can appear to possess them (Fig. 2I). In a growth series of leaves of *A. konjac*, developing druses were absent from the youngest leaves. As the leaves matured druses appeared initially only at the distal ends of the leaves, near the tips, but later small druses appeared also at the proximal ends of the leaves. Varying druse size and quantity gradients were apparent, with the largest druses and the greatest concentration occurring at the distal tip of the leaves (Fig. 2F and G, which are at the same magnification: druses at the leaf tip are much larger than those at the base). Similarly, in mature specimens of *A. variabilis* the greatest number and largest size of druses were concentrated at the very distal tip but were absent from the majority of younger leaves. In young leaves of *A. krausei* druses were absent near the leaf bases, but were again present near the tips. Small druses were also seen along the veins. As the tissues aged, druses also formed at the proximal ends. In general, druses were most commonly found at the leaf tips, except in *A. salmoneus*, in which druses were present at the leaf bases and absent from leaf tips, and *A. sutepensis*, which lacks druses entirely.

Raphide idioblast development

(1) *Early stages: before crystal formation*. Prior to crystal development, the cells that will ultimately form idioblasts are of similar dimensions to surrounding mesophyll cells (Fig. 3A). They possess a nucleus and nucleolus of similar size to those of surrounding cells, but lack chloroplasts and starch, although these also may be absent from surrounding tissues. Plastids are simple with few internal membranes (Fig. 4A); they are of a similar size to those in surrounding cells. The cytoplasm is usually dense and contains Golgi bodies, mitochondria, endoplasmic reticulum, numerous ribosomes and sometimes several small vesicles (Fig. 4B, C).

(2) *Mid-stages*. At this stage, crystal idioblasts are much larger than surrounding cells (Fig. 3B–G), and therefore readily distinguishable. As at earlier stages, the cytoplasm is often dense and granular, containing a network of endoplasmic reticulum (ER), numerous mitochondria, Golgi bodies and undifferentiated plastids. The idioblastic vacuole is larger than those of adjacent cells and may appear reticular, i.e. composed of numerous discontinuous vesicles (Fig. 3B–D). Although some vesicles within the idioblast appear transparent, others contain discrete amounts of a stained substance that often appears linked to the vesicle membrane (Fig. 4E, F). Within the stained area, some structural order may be observed (Fig. 4F) and developing crystals may also be present (Fig. 4D, G). In these cases, the dark-stained material takes the form of strips of varying lengths, sometimes with tapering ends (Fig. 5A). Within the strips can be seen pairs of short lengths (approx. 100 nm) of a denser substance that span the complete width of the strips (Fig. 5B). We interpret each pair as a crystal chamber. The stained sides of a crystal chamber are most commonly in close proximity, approx. 15 nm apart. They often appear unconnected but in some cases faint boundaries are observed (Fig. 5B). Often the dark-stained material is absent and membranes linking the corners of the chambers can be seen (Fig. 5C, D). Prior to crystal formation, the chamber usually enlarges and encloses a concave structure (Fig. 5C, D) that is bounded by the crystal chamber on two sides and by faintly staining granular material along the concave sides. The concave structure spans the total distance across the crystal chamber but does not fill it in the perpendicular direction, and so appears columnar. Crystal precipitation is seen as a white area within the images because resin does not penetrate the crystal, which then falls out during sectioning.

Crystal formation initiates between the chamber sides. As crystal deposition occurs, a white area is observed within the chamber that initially has a roughly rectangular outline, sometimes with one or two concave sides (Fig. 5E, F), the concave sides always being perpendicular to the crystal chamber. The chamber sides appear to overhang the developing crystal, resembling wings on either side. The area within the crystal chamber is filled as crystal deposition progresses and the characteristic grooved appearance becomes more apparent (Fig. 5G, H). Crystal growth also occurs both laterally and transversely. Few longitudinal sections were obtained through the crystals, due to severe difficulties of sectioning the material in this orientation. Those that are shown identify chambers with needle-like morphology (Fig. 6A, B). The pointed ends of the chambers are often considerably elongated, and have the appearance of two, possibly flexible, membranes coming together (Fig. 6B).

Granular material is often present within the crystal groove (Fig. 6C, D). In *A. bulbifer*, invaginations of the tonoplast membrane are common (Fig. 6E) and vesicles containing a granular substance occur in the vacuole; occasionally they are in direct contact with the crystal chambers. The crystal membranes are not often apparent as mucilage may be present around the crystals.

(3) *Late stages*. In a mature idioblast the cytoplasm is often pressed around the sides of the cell by the huge crystal-containing vacuole (Figs. 3H, 6F). Small vacuoles still occur in the dense cytoplasm. In most cases the region around the raphides has a flocculent appearance, but occasionally the crystals appear to be surrounded by mucilage. At maturity the raphides are tightly packed together (Fig. 6G).

Druse idioblast development in Amorphophallus

Unlike raphide idioblasts, druse crystal deposition occurs in cells of similar dimensions and appearance to surrounding mesophyll cells (Fig. 7A, B). The cell cytoplasm is not dense but ER, mitochondria, Golgi and plastids can be seen; unlike raphide idioblasts the plastids sometimes differentiate into chloroplasts (Fig. 7H). The cell nucleus is not enlarged. The cytoplasm already possesses several large vesicles forming the vacuole and thus appears more vacuolated than it does at the corresponding stage of raphide formation. Druses are initiated as small crystals within one or several vacuolar vesicles in the cell cytoplasm (Fig. 7A, B). As with raphide formation, dark-stained material occurs within the vacuole and geometric outlines can be observed within (Fig. 7C–E). Crystal deposition takes place within these outlines. Fragments of membranes can be seen within larger crystal deposits (Fig. 7F).

As the idioblasts develop, the vacuoles appear larger and characteristic small, star-shaped druses can be seen within (Fig. 7G, H). There are one or numerous druses per vacuole at this stage (Fig. 8A). A variable amount of flocculent material is present around the developing crystals (compare Figs 7H and 8A). Often, pockets of membranous vesicles appear to accumulate around the druses (Fig. 8B, C). Crystalline deposition occurs in several areas around the main crystal (Fig. 8D).

In mature druse idioblasts the crystal-containing vacuole almost fills the entire cell, the cytoplasm being pressed up to the cell wall or forming small, isolated pockets (Fig. 8E); however, the nucleus often can still be seen. The crystal aggregate is covered by a membranous sheath, which can appear looped or laminated. Numerous crystal faces appear to be projecting at various angles. In addition, crystal projections appear to have formed directly from existing projections, giving the appearance of interlocking crystal faces (Fig. 8F). Flocculent material may be present

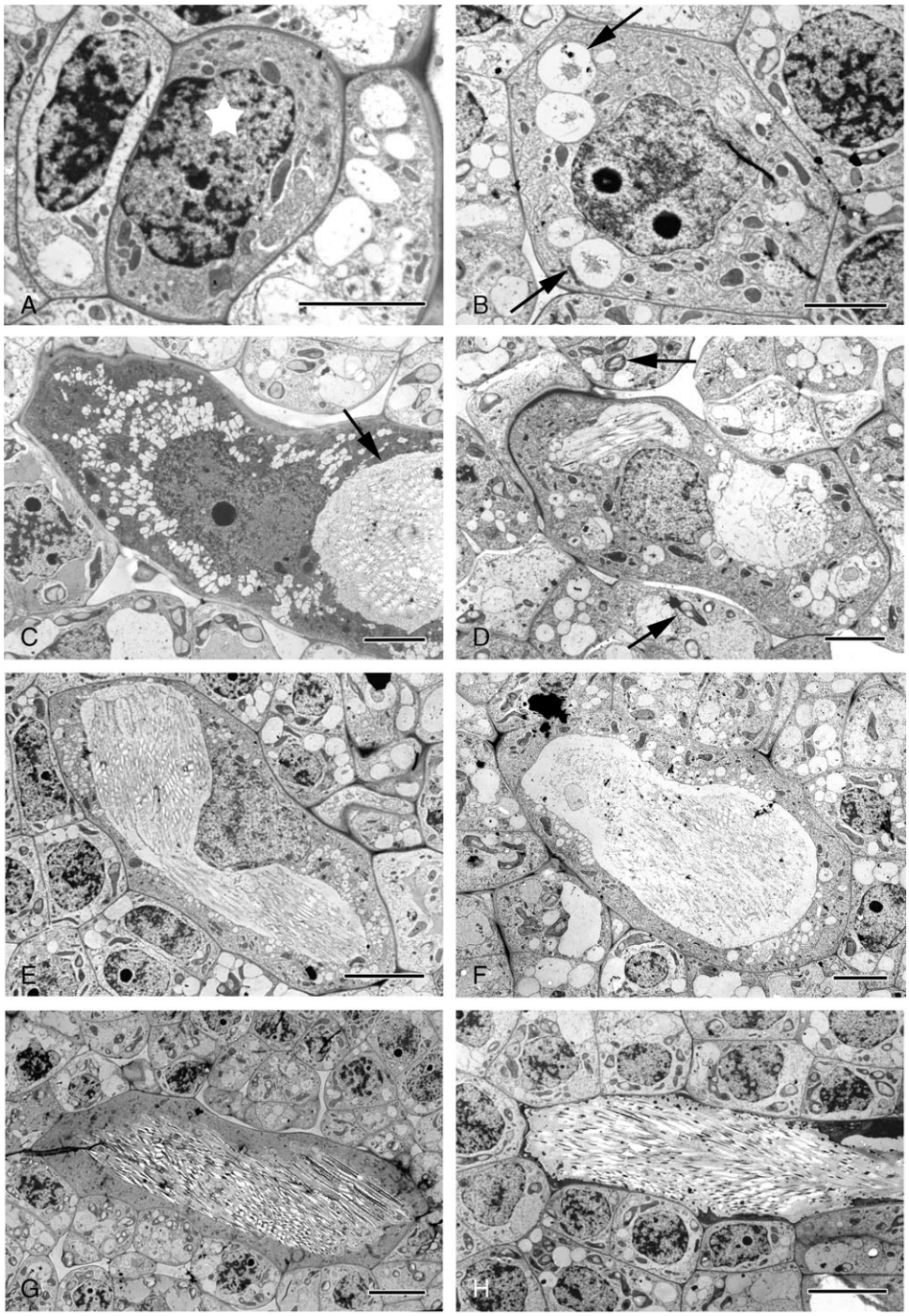

FIG. 3. *Amorphophallus variabilis*, TEM micrographs of raphide idioblast development illustrating how the proportions of the cell vacuole enlarges with respect to the overall idioblast dimensions as the crystals develop. (A) Potential pre-crystal idioblast (starred) possessing a densely staining cytoplasm. (B) Early stage raphide idioblast, several vesicles containing stained material present in cytoplasm (arrowed). (C) Mid-stage idioblast, much larger than adjacent cells. Crystals (white areas) have already formed in vacuole (arrowed). (D) Mid-stage idioblast. Chloroplasts possessing starch grains present in surrounding cells (arrowed). (E) At this stage the idioblast vacuole is large and contains stained material and developing raphides. (F) Small vesicles still appear in the idioblastic cytoplasm in addition to the large vacuole. (G) Late-stage idioblast, the vacuole containing numerous developing crystals. The cytoplasm is still densely stained. (H) The raphide-containing vacuole is large, with the cytoplasm pressed against the cell wall. Scale bars: (A–D, F) = 5 μm; (E, G, H) = 10 μm.

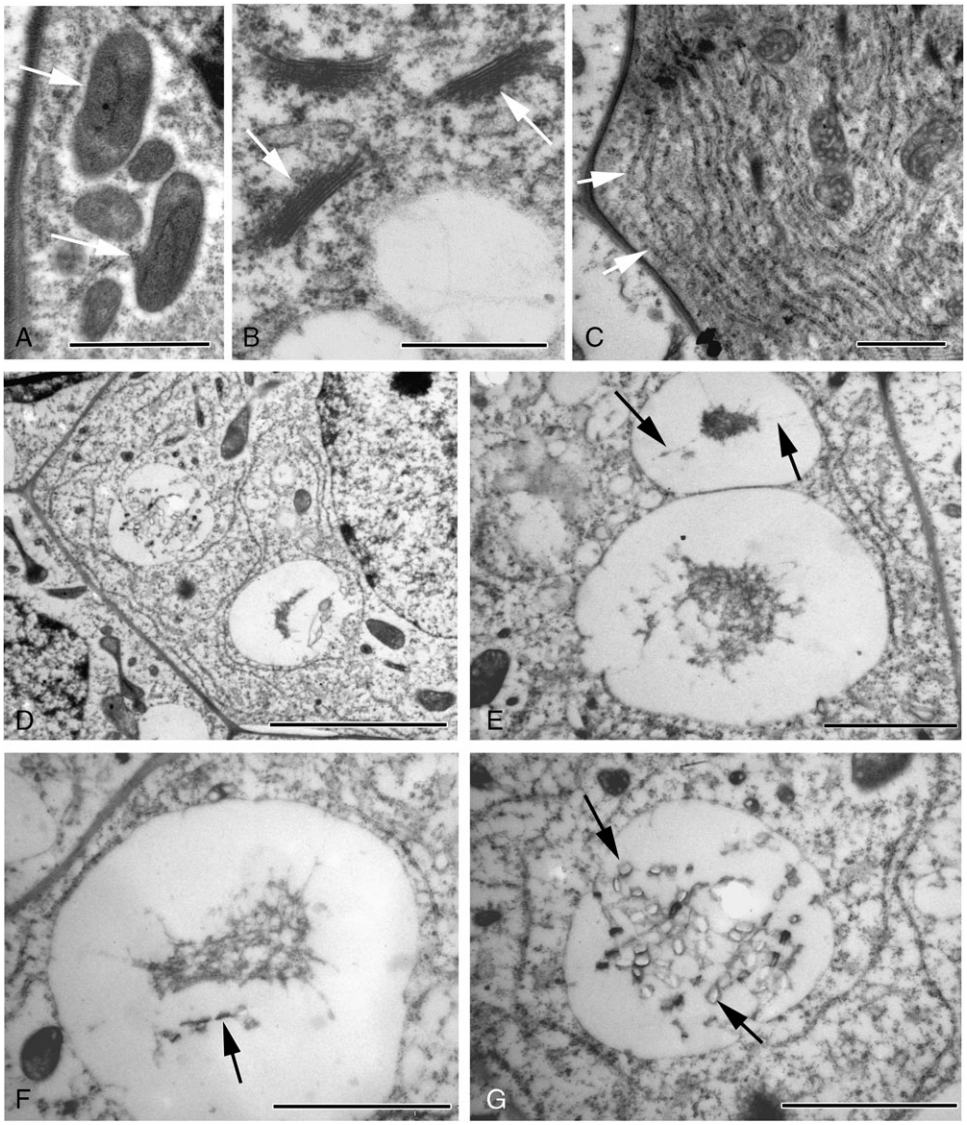

FIG. 4. TEM images of *Amorphophallus variabilis* leaf tissue. (A–C) Cytoplasmic organelles common in raphide cells, (D–G) Early raphide development. (A) Idioblastic plastids (arrowed) are simple, with little internal structure. (B) Numerous Golgi bodies (arrowed) and small vesicles are present. (C) Networks of rough endoplasmic reticulum occur (arrowed). (D) Vesicles containing stained material occur in cytoplasm. (E) The stained material occassionally appears to be attached to the vesicle wall (arrowed). (F) Ordered areas (arrowed) occur within the stained material. (G) Developing crystals (arrowed) are present in the vacuole. Scale bars: (A–C) = 1 μm; (D) = 5 μm; (E–G) = 2 μm.

throughout the vacuole. Occasionally, additional crystalline material is present in the same vacuole as a mature druse (Fig. 8E). Several small druses can develop within the vacuole of a single idioblast.

DISCUSSION

The unusual raphide groove that occurs within Araceae is a useful and consistent synapomorphy for the family (Prychid and Rudall, 1999). Furthermore, there is some variation in raphide morphology within Araceae, indicating that there could be further systematic potential. For example, our study shows that raphides in *Amorphophallus* resemble those of *Xanthosoma sagittifolium* (Cody and Horner, 1983), and some also possess barbs near their tips and along their edges, which occur in some other Araceae, such as *Colocasia*, *Alocasia* and *Pistia* (Sakai and Hanson, 1974; Kostman and Franceschi, 2000).

Differences between raphide and druse idioblasts maybe consistent with different levels of cellular regulation

The developmental timing, morphology, distribution and quantity of crystals within plant tissues is indicative of potential function. Our results support earlier hypotheses that raphides in *Amorphophallus* function both to deter herbivory (Volk *et al.*, 2002) and act in Ca sequestration and reabsorption under different environmental conditions (Franceschi and Horner, 1980; Franceschi, 1987, 1989), whereas druses primarily serve only the sequestration

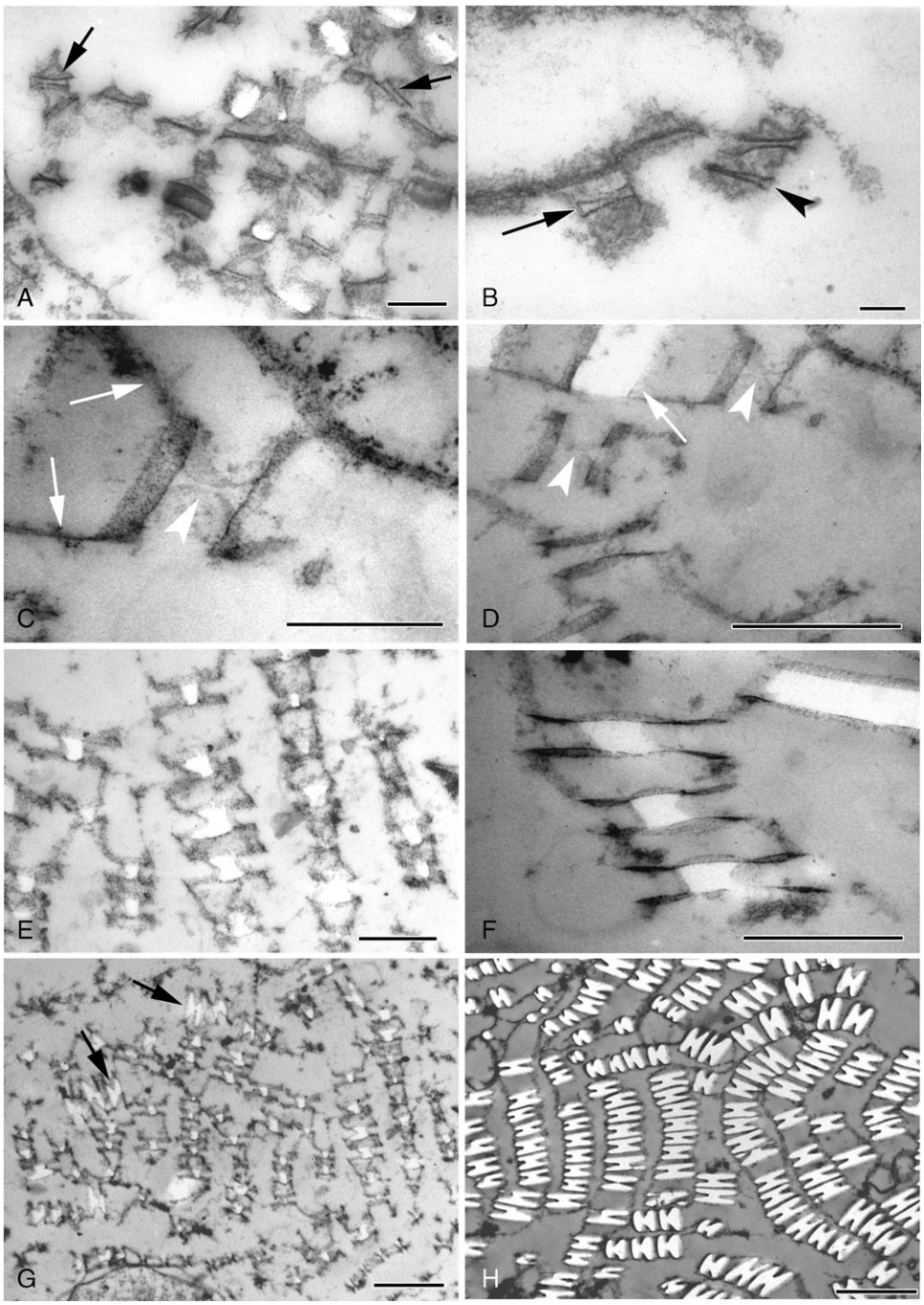

FIG. 5. TEM micrographs of transverse sections through developing raphide bundles within vacuoles in *Amorphophallus variabilis* (A–G) and *A. bulbifer* (H). (A) Early crystal formation, structural order occurs within the darkly stained material (arrowed). (B) Crystal chambers occasionally resemble closed four-sided structures (arrowed) or appear to possess two sides open to the tonoplast environment (arrowhead). (C) Membranes (arrowed) link the crystal chambers. Within the chamber a concave outline (arrowhead) can be seen prior to crystal deposition. (D) Concave outlines (arrowheads) within the crystal chambers. A larger raphide crystal is also visible (arrowed). (E) Early in development the crystals possess roughly rectangular cross-sections, sometimes with one or two concave sides. (F) Crystals are seen centrally placed within the crystal chamber. (G) Some crystals are starting to take on their characteristic H-shaped outline (arrowed). (H) Mature raphide crystals showing the H-shaped cross-section. Scale bars: (A) = 500 nm; (B) = 100 nm; (C, E) = 500 nm; (D, F, G) = 1 μm; (H) = 2 μm.

function. Franceschi and Nakata (2005) also suggested that developing raphides in *Pistia* could be involved with Ca regulation and mature raphides with defence; this could be the case here. However, these hypotheses may not be consistent with all crystal systems. In *Amorphophallus*, raphide formation occurs at very early stages of leaf development and tissue differentiation. Raphide idioblasts are generally regularly spaced apart and additional raphides are continuously initiated throughout the life of the tissues as they enlarge. Very young and actively dividing

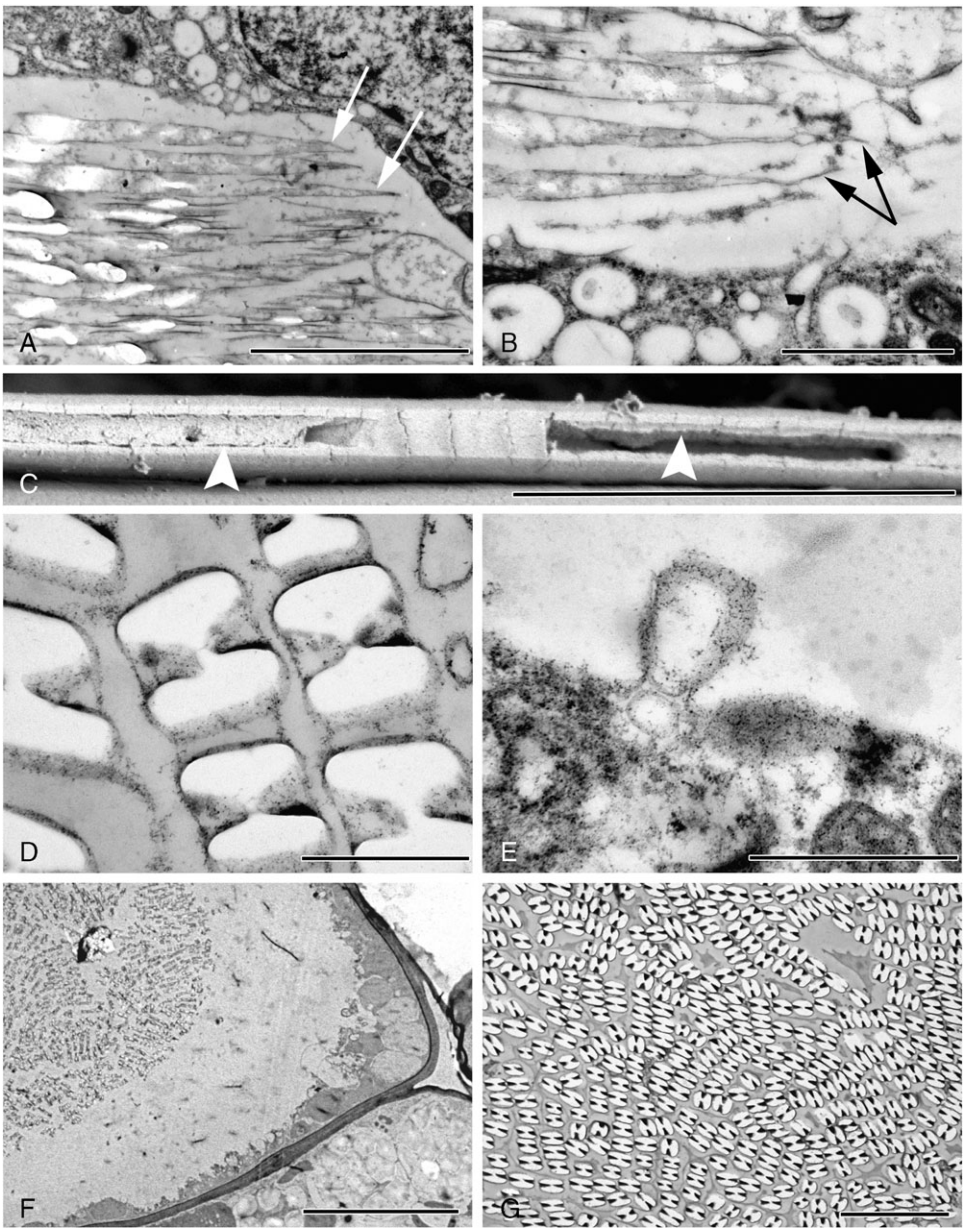

FIG. 6. Electron micrographs of raphide idioblasts in *Amorphophallus variabilis* (A, B), *A. taurostigma* (C) and *A. bulbifer* (D–G). (A) Longitudinal section through the crystal chambers, which have a needle-like outline (arrowed). White areas indicate locations of crystalline material. (B) In longitudinal view the ends of the crystal chambers are often considerably elongated (arrowed). (C) SEM image of one of the grooved sides of an individual raphide crystal. Material can be seen within the groove (arrowed). (D) Material can also be seen within the grooves of these raphides. (E) An invagination of the tonoplast. Similar vesicles are also found within the vacuole. (F) Raphide idioblast in endosperm tissue. Cytoplasm appears as a thin strip running along the cell wall. (G) Raphides occur packed tightly together in a mature idioblast. Scale bars: (A, C, G) = 5 μm; (B) = 2 μm; (D, E) = 1 μm; (F) = 10 μm.

cells have few vacuoles for dealing with Ca by intracellular sequestration; idioblast formation in these tissues could minimize the levels of Ca in adjacent cells, since dangerously high levels would affect regulation of biochemical and cellular processes and signal transduction pathways (Franceschi and Nakata, 2005). Regular raphide bundle spacing suggests that the idioblast acts as a Ca sink for a particular cell volume. The size of raphide as opposed to druse idioblasts means that much larger amounts of Ca can be sequestered in the former. Additionally, in times of Ca deficiency raphides have been shown to dissolve and release Ca required for cell growth (Tilton and Horner, 1980; Franceschi, 1987; Ilarslan *et al.*, 2001). Relatively early formation of raphides could also help to deter herbivores while the plant has not yet established secondary chemicals, textures or other defences against herbivory.

By contrast, druse crystals generally develop in older, differentiated tissues in *Amorphophallus* leaves, and have a more irregular distribution than raphides, being initially deposited at the leaf tips, as also in *Prunus serotina* (Lersten and Horner, 2006). The fact that the number of

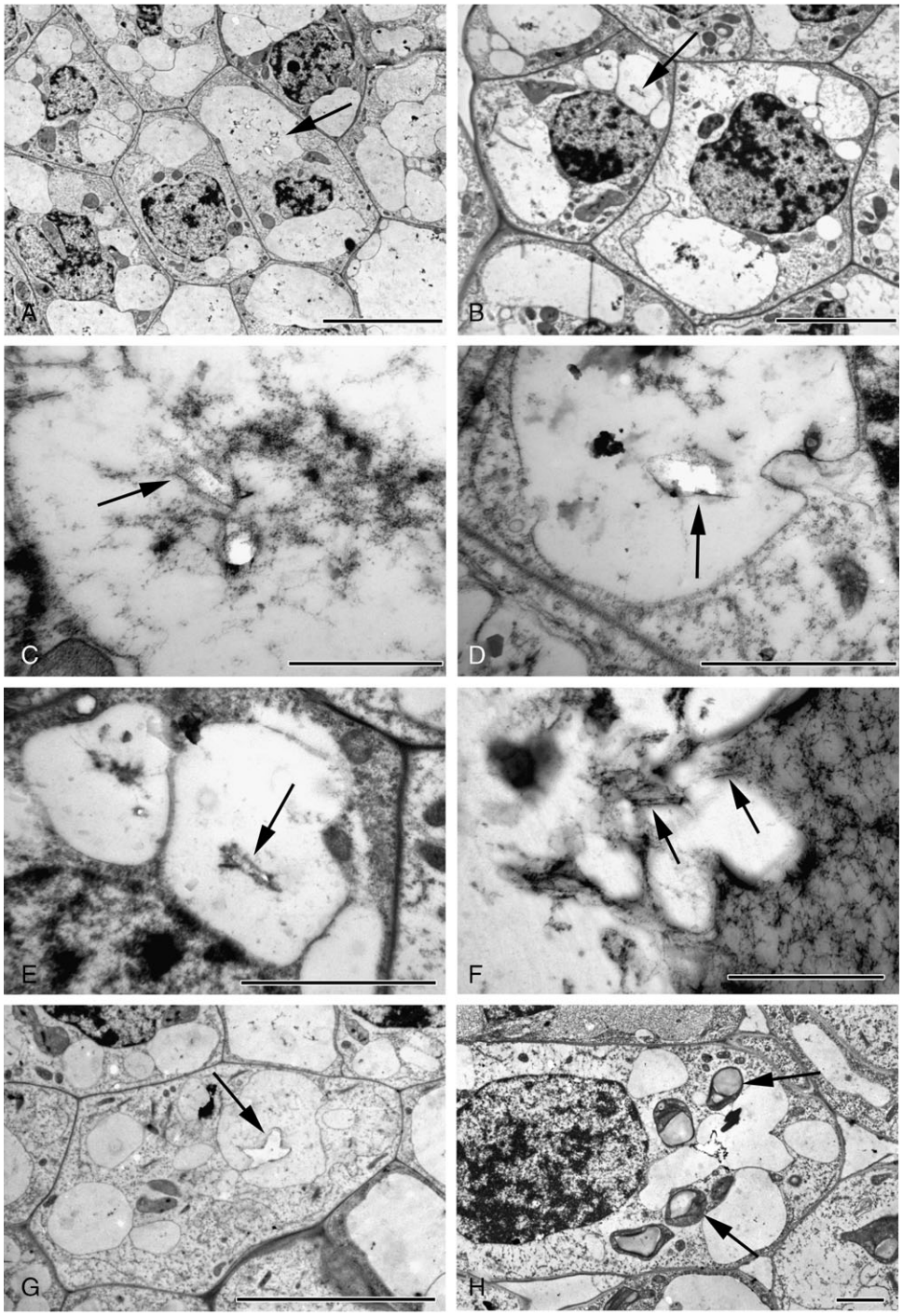

FIG. 7. Druse development, early and mid-stages in *Amorphophallus variabilis* (A–E, G, H) and *A. titanum* (F). (A, B) Druse idioblasts; note similar dimensions and appearance of idioblasts to adjacent mesophyll cells. Small crystals are present in the vacuoles (arrowed). (C–E) Vacuoles contain stained material within which faint geometric outlines (arrowed) may be seen. White areas denote crystalline material. (F) Pockets of vacuolar material; some with the appearance of membranous structures (arrowed) occur within the developing druse. (G) Small druse with its characteristic star-shaped outline (arrowed). (H) Druse idioblast possessing differentiated plastids, in this case chloroplasts possessing starch grains (arrowed). Scale bars: (A, G) = 10 μm; (B) = 5 μm; (C, F) = 1 μm; (D, E, H) = 2 μm.

druses can be enormously high, with almost every cell possessing them, indicates that raphide idioblast development is more strictly controlled. The positioning of druses in specific regions, with size and concentration gradients, may reflect the environmental conditions during plant growth that govern transpiration rates, and the amounts of calcium taken up by the plant at that specific point in development.

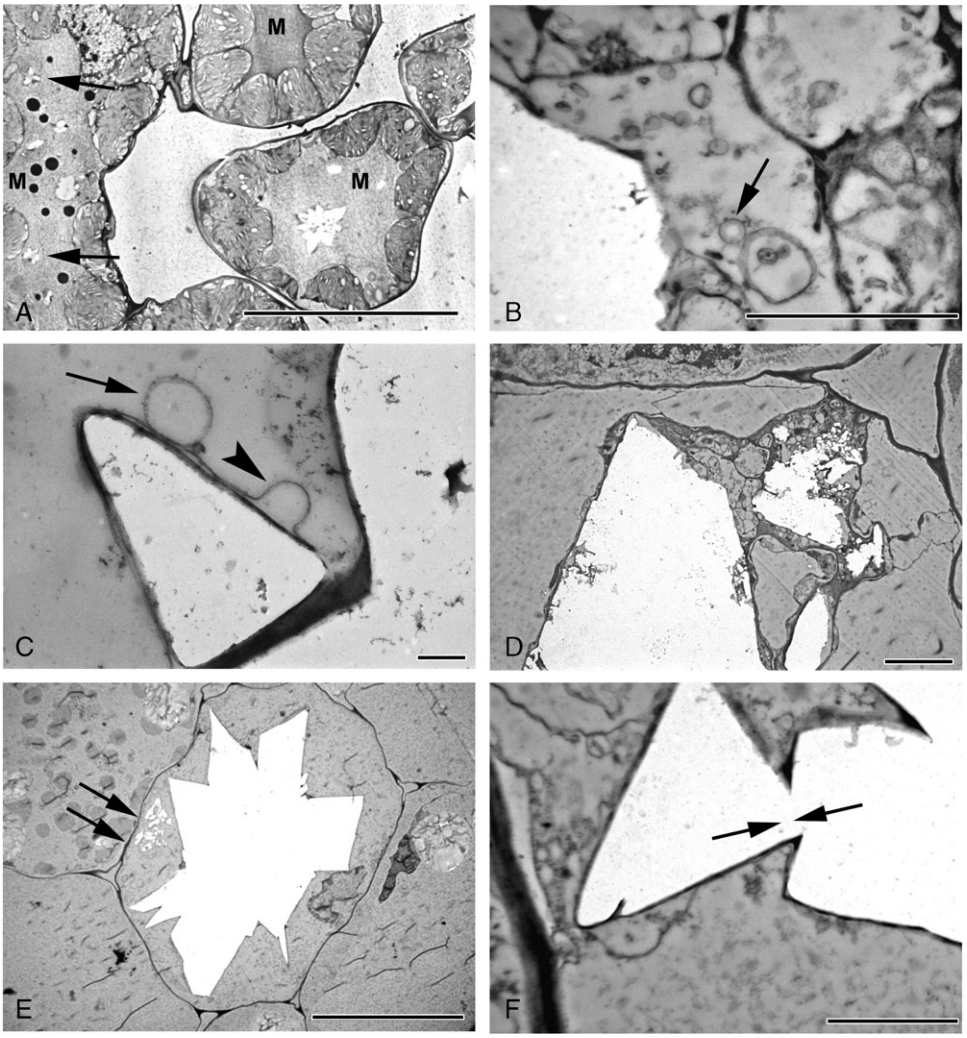

FIG. 8. Druse development, mid- and late stages in *Amorphophallus titanum* (A) and *A. krausei* (B–F). (A) Multiple druses (arrowed) developing in an elongated idioblast. Note stained mucilage (M) in vacuoles. (B) Numerous vesicles (arrowed) in close proximity to developing druse. Jagged edge of druse suggesting crystal deposition in steps or layers. (C) Membranous sheath around crystal face, often apparently looped (arrowhead). Vesicle (arrowed) in contact with sheath. (D) Crystal deposition occurring in several areas within the vacuole. (E) Mature druse, filling cell. Crystal deposition also seen (arrowed) in another part of the vacuole. (F) Crystal faces with differing orientations are interlocked (arrowed). Scale bars: (A, E) = 20 μm, (B) = 1 μm; (C) = 400 nm; (D) = 4 μm; (F) = 2 μm.

Druse idioblasts show less cellular differentiation prior to crystal formation than raphide idioblasts, again suggesting that raphide formation in *Amorphophallus* is a more regulated process, possibly requiring greater energy expenditure; this could be consistent with a greater functional level of importance. In our samples, druse idioblast precursors are indistinguishable from adjacent tissues, and do not appear to possess abundant organelles. In contrast, pre-crystal raphide idioblasts are more readily distinguishable by the dense cytoplasm, possessing undifferentiated plastids. Raphide precipitation seems to occur in already enlarged cells (as in *Psychotria*: Horner and Whitmoyer, 1972), suggesting that the cell differentiates into an idioblast; druse deposition occurs in cells that may not have developed specifically as idioblasts. However, since druse cells are living, druse development must involve energy expenditure by the cell and is, therefore, not merely a passive process.

Crystal deposition and raphide development could be governed by chamber structure

It is well known that raphides are formed within crystal chambers and this is also the case with *Amorphophallus*. In previous studies, crystal chambers in the aroid *Lemna* were shown to be closed rectangular structures (Mazen *et al.*, 2003), whereas those in the more distantly related eudicot *Vitis* were described as flexible tubular structures (Webb *et al.*, 1995). Raphide chambers in *Amorphophallus* are somewhat intermediate between these two conditions. They sometimes have a discrete rectangular appearance, but also often appear as two separate parallel

membranes, forming chambers apparently open to the surrounding dark-stained material or directly to the vacuolar contents (in Fig 5B compare the arrowed chamber with the non-arrowed ones). There are several possible explanations for this apparently intermediate condition.

(1) The chambers are rectangular structures but not all walls are distinct. The dense staining of the parallel walls of the chambers, as opposed to the mostly non-existent staining of the shorter perpendicular sides, could indicate that the latter have a different composition, or perhaps the wall components may have different orientations and so stain variably. A difference in wall composition might explain crystal or indeed groove formation; it has been shown *in vitro* that the addition of various compounds, such as peptides, glycoproteins, polysaccharides, lipids and organic acids, can promote or inhibit crystal precipitation and alter crystal morphology (Franceschi and Nakata, 2005; Dutour Sikirić and Füredi-Milhofer, 2006). A related possibility is that the chambers are initially rectangular but subsequently the shorter perpendicular walls fold back in on themselves, possibly as a result of different structural composition forming concave columnar structures prior to crystal deposition.

(2) Each crystal chamber could consist of two long, narrow, parallel membranous strips open to the vacuolar contents. Perhaps the membranes concentrate the vacuolar solution between them, producing a supersaturated solution that initiates crystal deposition, and/or perhaps nucleators are involved, particularly along the parallel surfaces, and hence deposition and crystal growth would be greater along the chamber walls, ultimately resulting in formation of the raphide groove.

(3) A third possibility is that the sides of the chambers were lost due to inadequate preservation. We consider this unlikely, because this would have affected all chamber walls, at least to some degree.

Thus, formation of the unusual raphide grooves along most of the crystal length is probably due to unusual crystal chamber morphology, either because the narrower faces of the crystal are not delimited by the chamber walls, or because the shorter walls have a different composition, restricting or promoting crystal deposition. Further work is required to isolate the chambers from the individual crystals to clarify this hypothesis. Li *et al.* (2003) also suggested that crystal nucleation and control of growth is governed by the chamber. Additionally, work is needed to determine whether crystal initiation is random, or occurs at a single specific point (nucleation site) within the chamber, or simultaneously at several specific sites. In the primary roots of *Yucca* and leaves of *Pistia*, raphide growth is suggested to be bidirectional (Horner *et al.*, 2000; Kostman and Franceschi, 2000). In our material, raphide growth could also be bidirectional, with the non-grooved mid-sections of the crystals acting as the initial sites of calcium oxalate deposition followed by crystal growth at both ends of the mid-section out along the elongated crystal chambers. The crystal chambers increase in size as the crystals enlarge, but it is not known whether crystal deposition actually causes the crystal chamber to enlarge or vice versa.

In contrast to the bidirectional growth that occurs in raphides, in druses calcium is deposited on all surfaces of the crystal simultaneously (Volk *et al.*, 2002). In *Cercidium floridum* (Price, 1970), *Capiscum annuum* (Horner *et al.*, 1981) and *Pistia stratiotes* (Volk *et al.*, 2002) the development of druse idioblasts involves membranes in the large central vacuole. In *Amorphophallus*, membranous sheaths are associated with the druses, and these appear to completely surround the developing crystals. Vesiculation of the cytoplasm could cause membranes or vesicles to be cut off into the vacuole, which then fuse with the membranes around the crystals. This could be the mechanism by which calcium and oxalate are added to the crystal surfaces, as in *Cercidium floridum* where druse sheaths are composed of membrane fragments originating from vesicles found in the vacuole (Price, 1970).

Multiple systems of transport into the vacuole

What transports the calcium or oxalic acid through the tonoplast into the vacuole? Could the vesicles that coalesce with the vacuolar membrane actively transport the soluble components needed for crystal formation, or do they simply increase the size of the vacuole for the developing crystals? In *Pistia* (Araceae), idioblast-specific Ca-binding proteins, potentially already bound to Ca, are transported to the vacuole in Golgi-derived vesicles and later incorporated into the raphides (Li *et al.*, 2003). In other Araceae, Mazen *et al.* (2003) demonstrated that Ca is associated with the stained material in the vacuoles and the Golgi vesicles, and proposed that the stained material contains a calcium-binding protein that is heterologous to the calcium-binding protein isolated from raphides of *Pistia stratiotes* (Araceae) by Li *et al.* (2003). Another Ca-binding protein, calreticulin, thought to be involved in regulating cellular Ca activity, has been found in *Pistia* ER; idioblasts are enriched with calreticulin relative to surrounding cells (Quitadamo *et al.*, 2000; Kostman *et al.*, 2003; Nakata *et al.*, 2003). In raphide idioblasts of *Amorphophallus*, ER and Golgi are present, but they are relatively sparse compared with those of secretory tissues, such as glands. There seems to be insufficient Golgi in our samples to cope with the massive induction of substances, such as oxalic acid, required to precipitate excess accumulated calcium, indicating that the crystal components may be transferred into the vacuoles by additional mechanisms, perhaps being pumped directly across the tonoplast from the cytoplasm.

We speculate that fusion of adjacent vesicles with the tonoplast could have caused thin strands of cytoplasm, tonoplast and vesicle membrane to become isolated or left projecting into the vacuole. These fragments would then form a component of the stained material around the crystal chambers and later the crystals themselves (compare the vesicle in Fig. 6E with the material within the crystal groove in Fig. 6D). Horner and Whitmoyer (1972) hypothesized that the crystal membrane complexes originate from the cytoplasm, plasmalemma and tonoplast. Wattendorf (1976) observed that even very thin layers of cytoplasm can deposit wall layers, and suggested that the

suberin-like sheaths around the crystals in *Agave americana* could have originated from thin strands of cytoplasm.

In summary, the uniquely grooved morphology of raphides in the family Araceae suggests that their crystal chamber morphology and composition differs from those found in all other plant families, probably resulting from an unusual crystal chamber morphology that becomes apparent at an early stage in crystal initiation.

ACKNOWLEDGEMENTS

We are grateful to Lin Jenkins, John Sitch and Marcello Solaro for their enthusiasm and expertise in growing the plants at Kew.

LITERATURE CITED

Arnott HJ, Pautard FG. 1970. Calcification in plants. In: Schraer H, ed. *Biological calcification: cellular and molecular aspects.* Amsterdam: North-Holland, 375–446.

Cody AM, Horner HT. 1983. Twin raphides in the Vitaceae and Araceae and a model for their growth. *Botanical Gazette* **144**: 318–330.

Dutour Sikirić M, Füredi-Milhofer, H. 2006. The influence of surface active molecules on the crystallization of biominerals in solution. *Advances in Colloid and Interface Science* **128–130**: 135–158.

Franceschi VR. 1987. Oxalic acid metabolism and calcium oxalate formation in *Lemna minor* L. *Plant, Cell & Environment* **10**: 397–406.

Franceschi VR. 1989. Calcium oxalate formation is a rapid and reversible process in *Lemna minor* L. *Protoplasma* **148**: 130–139.

Franceschi VR, Horner HT. 1980. Calcium oxalate crystals in plants. *The Botanical Review* **46**: 361–427.

Franceschi VR, Nakata PA. 2005. Calcium oxalate in plants: formation and function. *Annual Review of Plant Biology* **56**: 41–71.

Genua JM, Hillson CJ. 1985. The occurrence, type and location of calcium oxalate crystals in the leaves of fourteen species of Araceae. *Annals of Botany* **56**: 351–361.

Horner HT, Wagner BL. 1995. Calcium oxalate formation in higher plants. In: Khan SR, ed. *Calcium oxalate in biological systems*. Boca Raton, FL: CRC Press, 53–72.

Horner HT, Whitmoyer RE. 1972. Raphide crystal cell development in leaves of *Psychotria punctata* (Rubiaceae). *Journal of Cell Science* **11**: 339–355.

Horner HT, Kausch AP, Wagner BL. 1981. Growth and change in shape of raphide and druse calcium oxalate crystals as a function of intracellular development in *Typha angustifolia* L. (Typhaceae) and *Capsicum annum* L. (Solanaceae). *Scanning Electron Microscopy* **III**: 251–262.

Horner HT, Kausch AP, Wagner BL. 2000. Ascorbic acid: a precursor of oxalate in crystal idioblasts of *Yucca torreyi* in liquid root culture. *International Journal of Plant Science* **161**: 861–868.

Hudgins JW, Krekling T, Franceschi VR. 2003. Distribution of calcium oxalate crystals in the conifers: a constitutive defense mechanism? *New Phytologist* **159**: 677–690.

Ilarslan H, Palmer RG, Horner HT. 2001. Calcium oxalate crystal idioblasts in developing seeds of soybean. *Annals of Botany* **88**: 243–257.

Kausch AP, Horner HT. 1983. The development of mucilaginous raphide crystal idioblast in young leaves of *Typha angustifolia* L. (Typhaceae). *American Journal of Botany* **70**: 691–705.

Keating RC. 2003. *Anatomy of the Monocotyledons. IX. Acoraceae and Araceae.* (Series editors: Gregory M, Cutler DF.) Oxford, UK: Oxford University Press.

Keating RC. 2004. Systematic occurrence of raphide crystals in Araceae. *Annals of the the Missouri Botanical Garden* **91**: 495–504.

Kostman TA, Franceschi VR. 2000. Cell and calcium oxalate crystal growth is coordinated to achieve high-capacity calcium regulation in plants. *Protoplasma* **214**: 166–179.

Kostman TA, Franceschi VR, Nakata PA. 2003. Endoplasmic reticulum sub-compartments are involved in calcium sequestration within raphide crystal idioblasts of *Pistia stratiotes*. *Plant Science* **165**: 205–212.

Lersten NR, Horner HT. 2006. Crystal macropattern development in *Prunus serotina* (Rosaceae, Prunoideae) leaves. *Annals of Botany* **97**: 723–729.

Li X, Zhang D, Lynch-Holm VM, Okita TW, Franceschi VR. 2003. Isolation of a crystal matrix protein associated with calcium oxalate precipitation in vacuoles of specialized cells. *Plant Physiology* **133**: 549–559.

Mayo SJ, Bogner J, Boyce PC 1997. *The genera of Araceae*. Kew, London: Kew Publishing.

Mazen AMA, Zhang D, Franceschi VR. 2003. Calcium oxalate formation in *Lemna minor*: physiological and ultrastructural aspects of high capacity calcium sequestration. *New Phytologist* **161**: 435–448.

Nakata PA, Kostman TA, Franceschi VR. 2003. Calreticulin is an important component of the high capacity calcium sequestration mechanism in specialized plant cells. *Plant Biochemistry and Biophysics* **41**: 425–430.

Pennisi SV, McConnell DB. 2001. Inducible calcium sinks and preferential calcium allocation in leaf primordia of *Dracaena sanderiana* Hort. Sander ex M.T. Mast (Dracaenaceae). *Hortscience* **36**: 1187–1191.

Price JL. 1970. Ultrastructure of druse crystal idioblasts in leaves of *Cercidium floridum. American Journal of Botany* **57**: 1004–1009.

Prychid CJ, Rudall P. 1999. Calcium oxalate crystals in monocotyledons: a review of their structure and systematics. *Annals of Botany* **84**: 725–729.

Quitadamo IJ, Kostman TE, Schelling ME, Franceschi VR. 2000. Magnetic bead purification as a rapid, and efficient method for enhanced specificity of antibodies for immunoblotting and immunolocalization in plant samples. *Plant Science* **153**: 7–14.

Sakai WS, Hanson M. 1974. Mature raphide and raphide idioblast structure in plants of the edible aroid genera *Colocasia*, *Alocasia*, and *Xanthosoma*. *Annals of Botany* **38**: 739–748.

Sakai WS, Shiroma SS, Nagao MA. 1984. A study of raphide microstructure in relation to irritation. *Scanning Electron Microscopy* **II**: 979–986.

Thurston EL. 1976. Morphology, fine structure and ontogeny of the stinging emergence of *Tragia ramosa* and *T. saxicola* (Euphorbiaceae). *American Journal of Botany* **63**: 710–718.

Tilton VR, Horner HT. 1980. Calcium oxalate raphide crystals and crystalliferous idioblasts in the carpels of *Ornithogalum caudatum* (Liliaceae). *Annals of Botany* **46**: 533–539.

Volk GM, Lynch-Holm VM, Kostman TA, Goss LJ, Franceschi VR. 2002. The role of druse and raphide calcium oxalate crystals in tissue calcium regulation in *Pistia stratiotes* leaves. *Plant Biology* **4**: 34–45.

Wattendorf J. 1976. A third type of raphide crystal in the plant kingdom, six-sided raphides with laminated sheaths in *Agave americana* L. *Planta* **130**: 303–311.

Webb MA, Cavaletto JM, Carpitan NC, Lopez LE, Arnott HJ. 1995. The intravacuolar organic matrix associated with calcium oxalate crystals in leaves of *Vitis*. *Plant Journal* **7**: 633–648.